

Systematic search strategies in conformational analysis

Denise D. Beusen and E.F. Berkley Shands

Recent advances in the speed and accuracy of systematic search in conformational analysis have made it possible to address problems that just ten years ago would have been intractable or would have required an amount of time sufficient to compromise the utility of the results. This review focuses on systematic search and the authors' efforts to expand its utility through the development of novel strategies.

Over the last 20 years, the face of drug discovery has changed dramatically. Advances in molecular biology and biophysical methods¹ have enabled structure-based design², while combinatorial chemistry coupled with high-throughput screening^{3,4} has paradoxically all but obviated the need to know the structure of a therapeutic target. Yet with all of these changes, the simple fact that conformation and bioactivity are intimately coupled means that conformational analysis is still a basic tool very much in demand. The goals of these analyses remain what they have historically been: the identification of molecules and their conformations consistent with constraints derived from SAR or structural studies. The methods employed fall into several categories⁵: those that are random or stochastic (for example, molecular dynamics⁶, Monte Carlo⁷, distance geometry⁸), those based on heuristics and artificial intelligence⁹, and those that are systematic^{10–13}. Each of these diverse approaches to conformational analysis has an innate set of strengths and weak-

nesses with respect to its ability to sample comprehensively the conformations that are consistent with a set of limiting constraints.

Systematic search – concepts and limitations

The starting point for a traditional systematic conformational search is a rigid valence geometry: atoms are represented by hard spheres, and bonds by lines connecting the atoms; torsion angles are varied in regular increments and, at each conformation, every atom pair in the molecule is examined for steric contacts. The rigid geometry reduces the computational complexity and is experimentally justified by the smaller energetics of torsional deformation relative to bond-length and bond-angle distortion. While systematic search should be a path-independent means of conformational analysis that does not suffer from entrapment in local minima, there are practical considerations that dictate the thoroughness of its sampling. The error function is binary: that is, conformations are either kept or rejected depending on whether or not discrete interatomic distance constraints (experimentally derived or calibrated van der Waals¹⁴) have been violated. This contrasts with optimization protocols, such as molecular dynamics and distance geometry, where a continuous error function produces conformations over a range of energetic or distance violations. In systematic search, slight changes in the adjustable parameters can have a profound impact on whether or not distance constraints are violated. The most significant of these parameters (for a more complete discussion, see Refs 15,16) are the starting geometry, the van der Waals radii¹⁴, the value of the starting reference torsion angle, and the torsion angle increment. The first two affect sampling because perturbations in bond

Denise D. Beusen* and **E.F. Berkley Shands**, Center for Molecular Design and Department of Computer Science, Washington University, St Louis, MO 63130, USA. *Current address: Tripos Inc., 1699 S. Hanley Road, St Louis, MO 63144, USA. tel: +1 314 647 8837 ext. 3265, fax: +1 314 647 9241, e-mail: dbeusen@tripos.com or denise@ibc.wustl.edu

lengths and angles propagate as slight differences in inter-atomic distances, which in turn are evaluated against the experimental and van der Waals constraints. The last two parameters define the position and density of the sampling grid in torsional space. A sparse grid resulting from a large angle increment may fail to sample regions corresponding to local minima. A dense search grid could compensate for this shortcoming, as well as imperfections in the rigid valence geometry, by generating alternative valid conformations that are very close to a discarded point. Unfortunately, the explosive growth in the size of a calculation, with increases in the number of rotatable bonds and decreases in the torsion angle increment, limits the fineness of the search grid and the size of the molecules that can be analyzed. If A is the torsion angle increment, T the number of rotatable bonds, and N the number of atoms in a molecule, the total number of pairwise van der Waals evaluations during the course of a systematic search is given by Eqn 1:

$$\left(\frac{360}{A}\right)^T \times \frac{N(N-1)}{2} \quad (1)$$

Simply because of their sheer number, these van der Waals comparisons are the rate-limiting step in systematic search. Although the ever-increasing power of computer processors is essential in making systematic search feasible, algorithmic improvements for reducing the number of van der Waals checks, or enhancing the efficiency of performing these checks, are even more critical.

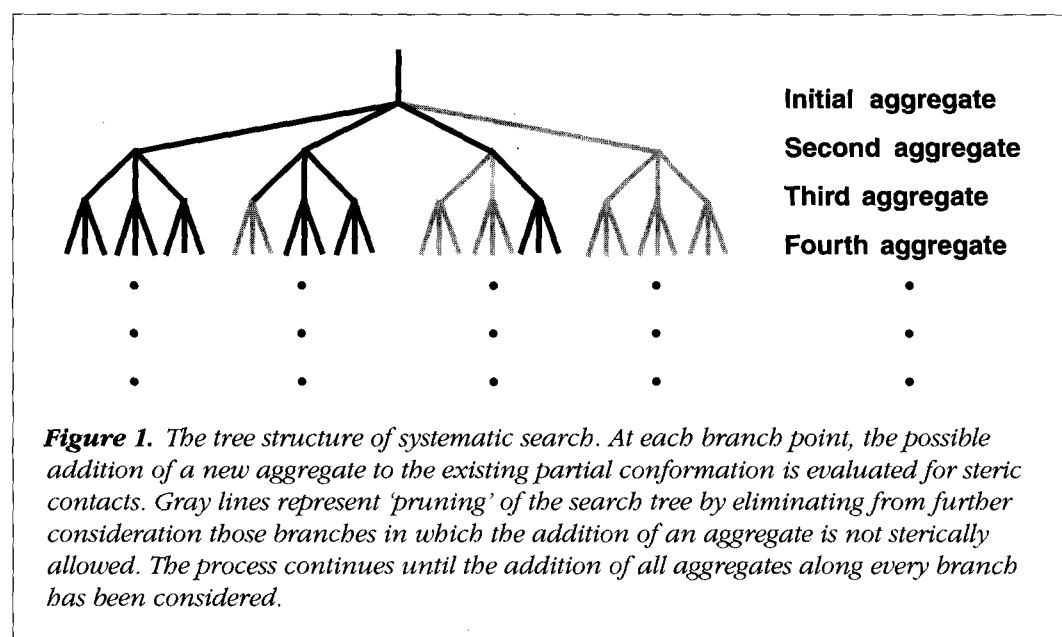
Strategies for enhancing the sampling properties of systematic search

A key element of our approach has been to avoid ‘brute force’ evaluation of the distances between every atom pair for every possible conformation of a molecule. As shown in Figure 1, the possible conformations to be evaluated can be represented in a search ‘tree’. The termini of the branches represent all of the possible torsional settings for the molecule. A significant reduction in computational complexity can be realized by determining at an early fork that a branch can be eliminated from further consideration. Our strategy (for a more complete discussion, see Refs 10,15–17) has been:

- To identify 'aggregates', which consist of sets of atoms whose pairwise interatomic distances are independent of torsional variations and consequently need to be evaluated only once;
- To employ a build-up procedure that involves the step-wise addition of aggregates;
- To use analytical methods to identify angle ranges in which a new aggregate could possibly be added at each branch point without steric overlap.

In our approach to systematic search, molecule construction and the determination of angle ranges that may contain sterically allowed conformers occur simultaneously. Analysis of torsion ranges that do not contain valid conformations is terminated (Figure 1).

Our analytical methods are based on equations that describe the variable distance between any two atoms as a function of a single torsion angle^{10,16,17}. For the addition of each aggregate, all of the pairwise atomic distances that span the torsion are evaluated. The allowed torsion ranges for addition of the new aggregate are intersected over all of these atom pairs and, from the resulting ranges, trigonometric tables are constructed that define points



on the sampling grid. These tables can be further refined by fixing a given torsion and applying the distance equations to the next downstream torsion: in effect, chaining the analytical method. If there are pharmacophore or experimental distance constraints, a 'look-ahead' procedure is used to further edit the trigonometric table before and during execution of the search. As shown in Figure 2, constrained atoms are projected onto preceding rotational axes to approximate new ranges for the constraints that can be used in the distance equations mentioned above. With the exception of cyclic structures, look-aheads extending beyond three rotatable bonds down the search tree do not significantly refine the allowed ranges for the initial rotatable bond.

There are a number of other techniques that we have employed to attack the combinatorial explosion. Redundant calculations, arising from evaluating the same adjacent aggregate contacts in all branches of the search tree (Figure 1), are eliminated by storing combinations of allowed torsion angles for subsequent recall. We employ divide-and-conquer strategies, which use multiple processors or divide large molecules into overlapping fragments whose search results are later recombined. The steric (Lennard-Jones) and torsional energies across each rotatable bond can be evaluated and those above a certain threshold eliminated to prune the search tree further.

Radial and adaptive sampling

Speed enhancements resulting from the strategies outlined above have allowed us to focus on improvements in the sampling properties of systematic search. When there are large variations in the number of fixed (non-rotatable) bonds that separate atom pairs, over- or undersampling of Cartesian and distance space can occur. This situation is represented in Figure 3a, where the rotating arm lengths of a methyl hydrogen and a phenyl hydrogen are compared. With a uniform angle increment of 10° , the much larger three-dimensional space swept by the hydrogens of the phenyl group would be undersampled relative to that of the methyl group. The solution we have implemented is *radial sampling*, in which the sampling grid is constructed in distance space, thereby compensating for differences in arm length. In Figure 3b, the strategy for calculating the distance grid and converting it to torsion angle space is illustrated. In each aggregate, a key atom is selected. These are pharmacophore atoms (when present) or the reference atom of the subsequent torsion. The distance (d_0 or d_1) from

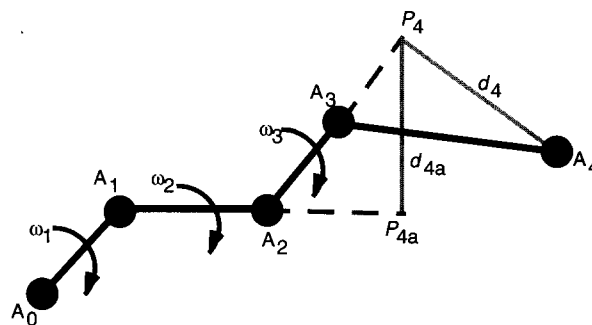


Figure 2. Analytical determination of torsion-angle ranges that may contain allowed conformations. A_0 – A_4 represent aggregates within which interatomic distances are invariant. Addition of each aggregate is sequential, with analytical determination of allowed ranges for the torsion separating the aggregates (i.e. possible ranges of ω_1 in which A_1 can be added to A_0 without steric contact, etc.). Once ranges of ω_1 that may contain allowed conformers are determined, then it can be fixed at each of several grid points and the allowed ranges for ω_2 calculated in a similar fashion; branches of ω_1 for which all ω_2 ranges are invalid are dropped from further consideration. Look-ahead is a process by which settings of ω_1 are similarly pruned by determining the allowed ranges for angles two or more torsions away. In this case, A_4 is an aggregate whose rotation is controlled by ω_3 and which contains an experimental or pharmacophore constraint to A_0 . In order to determine ranges of ω_1 that are consistent with the constraint between A_0 and A_4 , the constrained atom in A_4 is projected onto the ω_2 axis (P_4), and this projection is in turn projected onto the ω_1 axis (P_{4a}). The A_0 – A_4 distance constraint is expanded by $d_4 + d_{4a}$ and used in the distance equations to find allowed torsion ranges for ω_1 .

the key atom to the axis (ω_0 or ω_1) governing the rotation of its aggregate is determined, and the circumference of the rotation circle of the key atom is divided into arcs of equal length. Torsion angle values that move the key atom by the user-specified uniform arc length are then calculated. With radial sampling, each torsion has a unique floating-point angle increment.

Adaptive sampling is our approach to limitations in sampling that result from a fixed search grid. For a given torsion, the ranges that possibly contain valid conformations vary in width as they are the intersection of the allowed angle

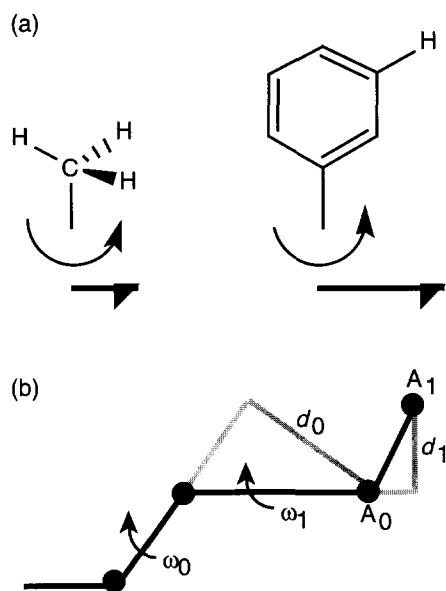


Figure 3. Radial sampling. (a) Comparison of the rotor arm length for hydrogens bonded to a methyl group (left) and a phenyl group (right). When uniform torsional grid sampling is used, the difference in arm length means that the hydrogens in each group sample both distance and Cartesian space differently. (b) Geometric parameters used to calculate radial samples for systematic search. A_0 and A_1 are key atoms in the aggregates whose rotation is controlled by ω_0 and ω_1 , respectively. Key atoms are projected onto their rotation axis in order to determine the radius of their rotation circle (d_0 and d_1 , respectively). The circumference of the rotation circle is divided into user-specified equal-length arcs. Floating-point torsion angle increments, which move the key atoms by the arc distance, are then calculated.

ranges for all nonbonded atom pairs across that torsion. A typical situation is shown in Figure 4, where possible angle ranges for sterically allowed conformations are represented by shaded boxes. In Figure 4a, the leftmost box represents a range that is not sampled at all using conventional grid-based sampling, and the rightmost box is an allowed range that is inadequately sampled. Adaptive sampling is shown in Figure 4b, where grid points are moved to ensure that all allowed ranges are adequately sampled. By determining the sample points dynamically, adaptive sampling abandons the concept of a fixed grid. Our experience¹⁸ is that adaptive sampling produces more complete results than the fixed grid approach. Because the equations discussed earlier relate interatomic distances and the torsion separating them, the concept of adaptive sampling can be applied not only to torsional grids, but also to distance (radial) grids.

Systematic search applications

Constrained search – the active analog approach

The aim of the active analog approach¹⁹ is to deduce the three-dimensional arrangement of key interaction sites in a receptor–ligand complex from the sets of conformations accessible to a series of high affinity, flexible ligands. Constrained Search¹⁷ is a program that implements the active-analog approach by finding the logical intersection of all possible interpharmacophore distances across all sterically allowed conformations of a set of ligands. The binding site geometries are represented as points in distance space, where each dimension represents an internuclear distance between two atoms in different pharmacophoric groups.

As a basis for our development of Constrained Search, we have worked with the set of 28 angiotensin-converting

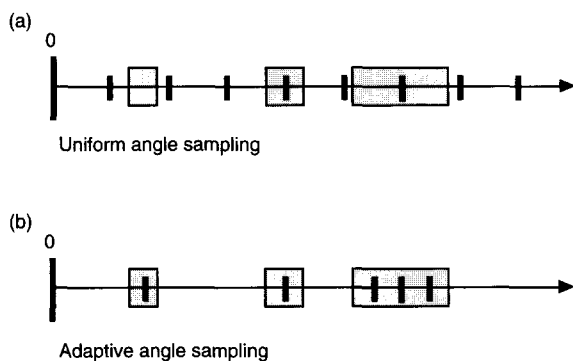


Figure 4. Schematic representation of adaptive sampling. (a) Possible allowed angle ranges are determined by the distance constraint equations for every atom pair across a given torsion. Intersection of these ranges yields fragments of torsional space (gray boxes) that may not be sampled at all (leftmost box) or are inadequately sampled (rightmost box). (b) By repositioning the grid points to sample the allowed angle ranges, more comprehensive sampling results. The horizontal arrow represents the entire range of torsion angles from 0° to 360°; possible sterically allowed torsion ranges are represented by the gray boxes. The vertical bars represent grid points.

enzyme (ACE) inhibitors originally analyzed by traditional systematic search²⁰. That study employed 10° angle increments with fixed rings and, with the exception of a zinc site, measured only intraligand distances. Our first version of Constrained Search¹⁷ employed the same paradigm, but made these analyses essentially interactive by:

- Including heuristics for ensuring that the most constrained molecules are searched first and thereby pruning search trees early in the analysis;
- Early termination of the search of a given molecule when all of the previously known points in distance space had been found;
- Eliminating exhaustive evaluation of all conformational possibilities for pendent groups that are not on the path of torsions directly connecting the pharmacophoric groups.

Subsequently, we augmented the ACE inhibitor model to include more receptor site points on the ligands (and the associated additional degrees of freedom), and applied radial and adaptive sampling^{18,21}.

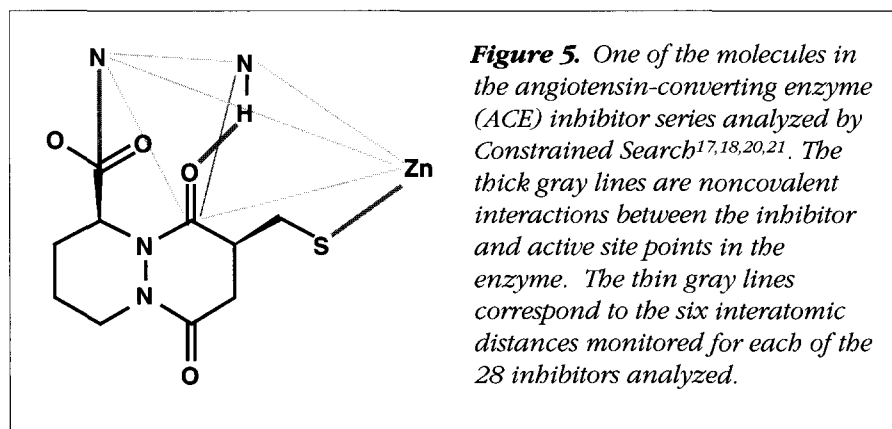
Our current version of constrained search (RECEPTOR 3.2, Tripos Inc., 1699 S. Hanley Road, St Louis, MO 63144, USA) is 100 times faster than our previously reported version¹⁷ and 10⁷–10¹² times faster than the equivalent systematic search (SYBYL 6.2, Tripos Inc., 1699 S. Hanley Road, St Louis, MO 63144, USA). The speed of our analyses (for all 28 molecules, approximately 5 min on a DEC Alpha 3000/300 work station) has made it feasible to do multiple analyses of the same ligand dataset to probe the impact of adjustable parameters on the search results¹⁸. We now routinely allow rings to flex and perform searches in very small increments (1–6°). The pharmacophore distances monitored in these searches are shown for one of the ACE inhibitors in Figure 5. In Figure 6, a sample of the allowed conformations of this molecule are overlaid. Figure 6a shows the results of a conventional systematic search done with fixed torsional grid sampling in 11° increments; Figure 6b shows the results of a radial adaptive sampling analysis done with a radial increment of 0.25 Å (average torsional increment of 11.2°). In our analyses¹⁸, we find that radial sampling is more comprehensive than torsion angle sampling, and that adaptive sampling is more complete than simple

grid-based sampling. Radial adaptive sampling combines both of these enhancements and is the most efficient approach of all.

We have also applied Constrained Search to a set of approximately 30 high-affinity substance P (SP) antagonists (Y. Takeuchi, E.F.B. Shands and D.D. Beusen, unpublished), which represent the diverse classes of SP antagonists²². These molecules generally consist of two aromatic rings, which can be linked to a quinuclidine²³ or a piperidine²⁴ core; in other cases, they are tryptophan esters/amides²⁵ or perhydroisoindols²⁶. A π - π interaction between the two rings has been postulated in the bound conformation of these ligands^{24,25,27,28}. Methoxy or trifluoromethyl substituents on one of the rings and/or a heteroatom in the region of the molecule linking the two rings are also thought to be important for binding^{23,29}. Our results revealed that only edge-to-face orientations of the two phenyl rings were common to all of the classes of antagonists. These analyses, done with all of the cyclic structures completely flexible and using a radial increment of 0.0625 Å (equivalent to an average torsional increment of 2.66°) required 1 computer processing unit (CPU) day on a Dec Alpha 3000/300. An overlay of four members of the piperidine class of antagonists is shown in Figure 7.

Ringsearch: conformational analysis of cyclic molecules

Covalent, cyclic constraints are used to limit the flexibility of ligands and to test hypotheses about the bound conformation of the ligand³¹. A variety of conformational analysis tools have been applied to cyclic systems^{13,32–34}. In one study³⁵, a single systematic search was used to identify trial conformations of caprylolactam, a nine-membered ring, which were subsequently optimized using the MOMO force



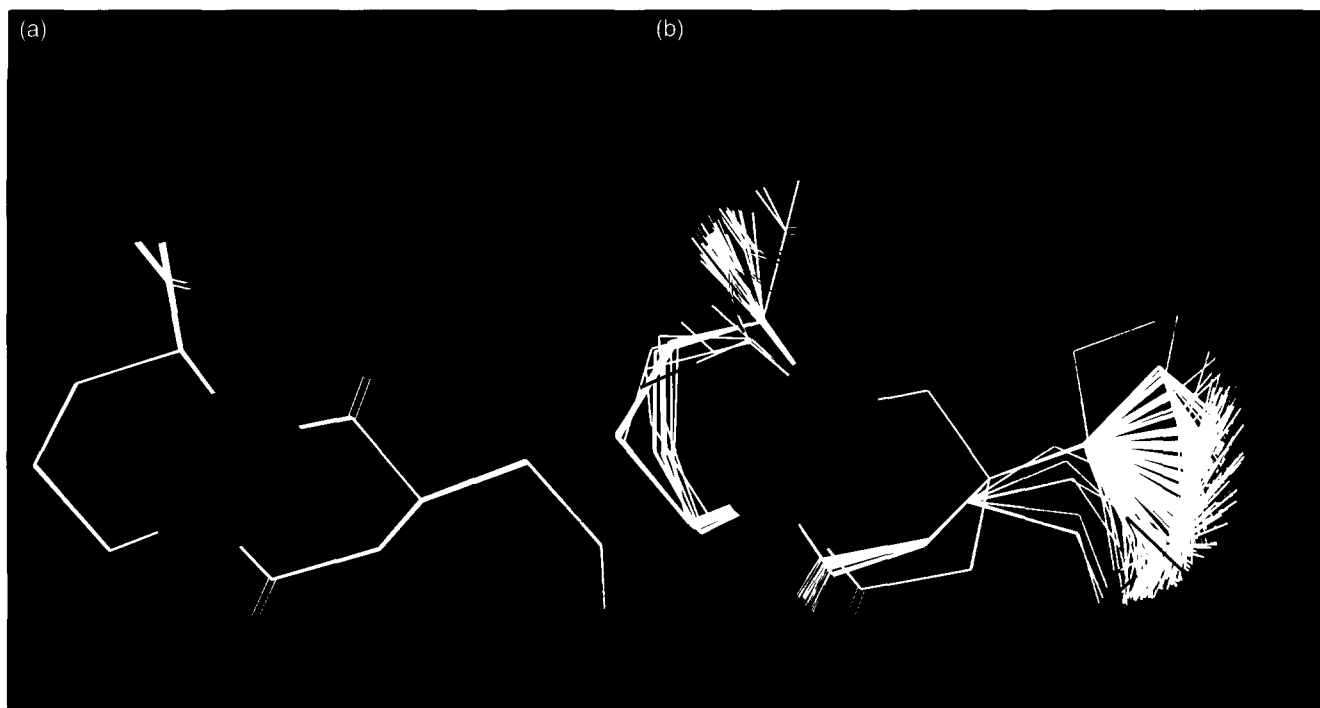


Figure 6. Overlaid conformations of the molecule shown in Figure 5 generated by Constrained Search. (a) A fixed torsional grid search at 11° increments produced two points in distance space common to all of the angiotensin-converting enzyme (ACE) inhibitors. Only 12 conformers (all shown) were consistent with the two points. (b) A radial adaptive sampling search (average angle increment 11.2°) generated 3345 points (12 clusters) in distance space. A single conformer was selected for each point and these were clustered into 178 families, from which 458 conformers (shown here) were selected as representative based on RMS_{tors} comparison. Atom color key: carbon, white; sulfur, yellow; zinc, pink; nitrogen, blue; hydrogen, light blue; oxygen, red.

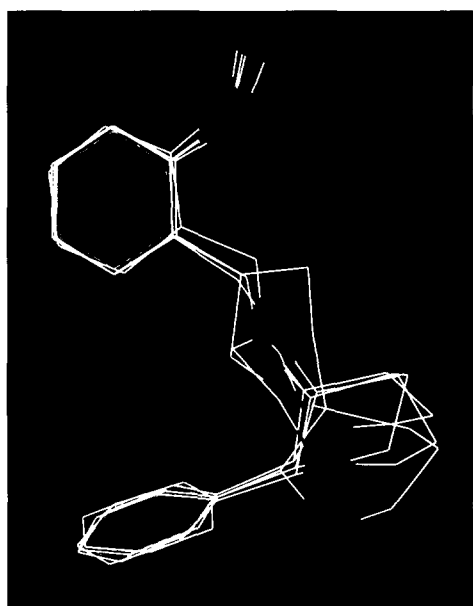


Figure 7. The alignment of four substance P (SP) piperidine antagonists determined from a Constrained Search analysis of about 30 SP antagonists of different chemical classes. The molecules shown are CP 99994 (Ref. 24), structure 3 of Ref. 28 and structures 4a and 7a of Ref. 30. Atom color key: carbon, white; nitrogen, blue; oxygen, red.

field. The authors concluded that systematic search was less efficient and less complete than molecular dynamics and Monte Carlo in finding 39 caprylolactam minima. Our group (M. Yodo, T. Kataoka and G.R. Marshall, unpublished) and others³⁶ have concluded that this force field produces high-energy minima that are not true minima on the MM2 energy surface and are unlikely to be found valid in systematic search. We have recently revisited this problem using our latest tools. The analytical methods that figure so prominently in the efficiency of our search algorithms are readily adaptable to the solution of cyclic structures. In the process of adding aggregates to construct the cycle, geometric constraints extracted from the starting structure (either linear or cyclic) are used to solve for conformers in which the ring-closure bond and

angle are precisely defined. Because the torsion grid is so fine and because we are able to use tight closure tolerances, the resulting conformations are generally very close to the nearest local minimum.

In Table 1, the results from four different types of searches are compared: a fixed torsional grid search, a fixed radial grid search, an adaptive torsional search and an adaptive radial search. In each case, the resulting dataset was first sorted into families in torsion space and then each family was filtered using an torsion root mean square (RMS_{tors}) criterion to identify unique representative conformers. When the MM3-minimized representative conformers were compared with one another, a total of 53 unique minima were identified, all within approximately 14 kcal of each other. Within any given search, it was generally the high-

energy minima that were missed. The times listed in the table clearly show the speed of our search protocols, with all but one under 45 min. The ratios of CPU to elapsed time for the searches average 5.5, which is 91% of the predicted speed-up using six of the eight processors on an SGI 4D/380. These results confirm our findings from ACE inhibitor analyses¹⁸: namely, multiple searches, done under a variety of protocols and parameters, are essential for accurate conformational analysis.

Macrosearch: generation of structures from NMR-based restraints

Macrosearch is a program that makes systematic search feasible for generating initial structures of peptides and proteins from NMR data. These can then be optimized

Table 1. Summary of unconstrained systematic searches of caprylolactam^a

Search type	Angle increment or its equivalent	van der Waals scale factors ^b	Search CPU time	CPU/elapsed	Number of conformers	Number of families ^c	Family sorting CPU time	% RMS_{tors} scaled ^d	Number of samples	Number of MM2 minima found ^e
Fixed angle	5	0.95, 0.87, 0.65	21:03.84	5.333	5944	277	00:11.83	100	455	42
Fixed radial	5	0.95, 0.87, 0.65	20:26.32	5.286	6152	240	00:11.35	100	404	43
Adaptive angle	5	0.95, 0.87, 0.65	31:42.13	5.628	61932	62	06:18.08	50	503	46
Adaptive radial	5	0.95, 0.87, 0.65	30:18.94	5.546	63038	47	05:42.06	50	282	40
Adaptive radial	4	0.85, 0.77, 0.65	01:34:40.53	5.808	285796	23	01:21:14.89	75	527	45
Adaptive radial	5	0.85, 0.77, 0.65	44:18.66	5.504	87870	49	11:07.40	50	514	44
Adaptive radial	6	0.85, 0.77, 0.65	20:43.96	5.271	26766	159	01:34.58	100	309	40

^aSet-up parameters: reference torsion, absolute; starting geometry, MM2-minimized X-ray coordinates (refcode = CAPRYL, Ref. 37); calibrated radii¹⁴ with H radius reduced by half; amide range searched, *cis* and *trans* $\pm 45^\circ$; ± 0.05 Å closure bond length tolerance; $\pm 8^\circ$ closure bond angle tolerance. These two tolerances correspond to localized strain energies of about 1.5 kcal.

^bThese scale factors are applied to all atoms uniformly. The first factor scales all pairwise distance constraints; the second scales distance constraints between atoms having a 1,4 relationship; the third scales atom pairs that can hydrogen bond.

^cFamily analyses were done on a DEC Alpha 3000/300, with a processor approximately three times faster than any individual processor on the SGI 4D/380 used for the searches. A family is defined as any cluster of points in torsional space that is unconnected to any other cluster by contiguous points on the search grid.

^dAfter clustering into families, the midpoint of the allowed angle range for every rotatable bond in the cluster is determined. The average RMS_{tors} for every conformer against that value is calculated. Conformations within a threshold value of this RMS_{tors} (50%, 75%, or 100%) are removed from consideration, and a new average RMS_{tors} is calculated from the remaining conformers. The process is iterated until no more conformers remain in the family.

^eA total of 53 unique minima was found over all searches.

against a molecular mechanics force field augmented with NMR-based distance or nuclear Overhauser effect (NOE) intensity restraints. There are several advantages to a systematic search strategy for generating NMR structures. Because systematic search returns results only when constraints are satisfied, there are no constraint violations in the structures produced. The explicit enumeration of all conformational possibilities precludes entrapment in local minima that do not satisfy all of the experimental constraints. Constraints can be implemented in a hierarchical fashion, with longer-range constraints implemented only when short-range constraints have been satisfied, and as a result there is no homogenization of data with constraints compromised in order to satisfy others. Because a rigid, reasonable geometry is employed, the question of how the experimental constraints perturb force field terms is not an issue.

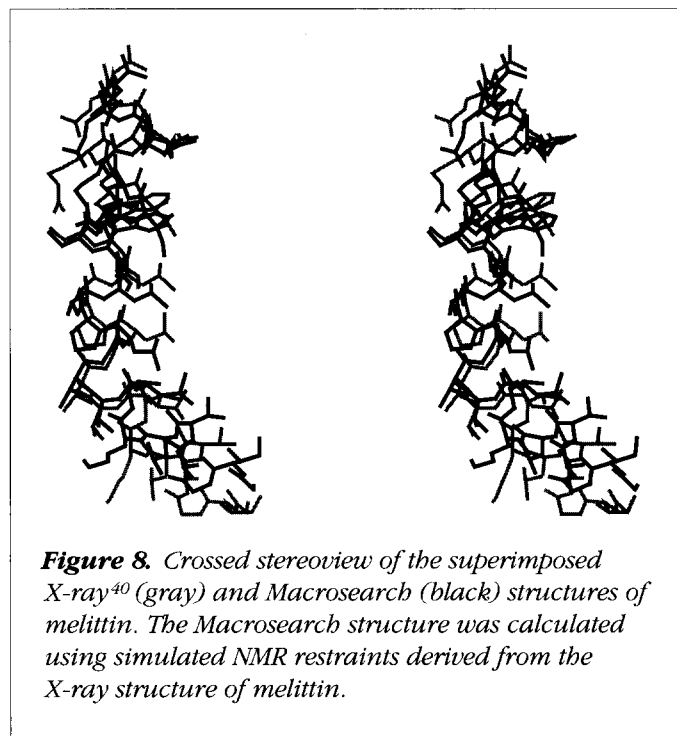
Initially, conformational searches within Macrosearch are performed on individual residues. The results are then used to create new input files consisting of overlapping multiresidue fragments of the original molecule. These files contain all associated distance restraints and limit the accessible torsion angle ranges to only those found to be valid in individual residue searches. The two-tiered strategy of Macrosearch makes it possible to do stereospecific assignments^{38,39} for individual residues, and speeds the search of the larger fragments by eliminating from consideration torsion ranges that are inconsistent with short-range restraints. The results for each fragment are grouped into families and the ranges of overlapping angles in each family of a fragment are intersected with those of the adjacent fragments. Families from neighboring fragments that do not have intersecting or contiguous angle ranges in the overlapping torsions are dropped from further consideration. This overlap evaluation is done throughout the length of the sequence, resulting in several superfamilies from which a representative conformation is selected.

To test Macrosearch, 248 distance constraints were extracted from the X-ray structure of melittin (26 residues⁴⁰), an error range of $\pm 15\%$ was applied to each, and all were used to constrain a systematic search along with the coupling constant for the NH- α H interaction ($J_{\text{NH-}\alpha\text{H}}$) calculated from the observed ϕ angles. Fragments consisting of four residues were used with a two-residue overlap, and torsions were evaluated in 10° increments for the backbone and 30° increments for side chain torsions.

Table 2. Summary of Macrosearch results for melittin^a

Fragment	Conformations	Families
0	25,610	1
1	6,562	6
2	75,000	1
3	75,000	9
4	151	3
5	78	1
6	230	1
7	15,637	2
8	211	1
9	2,404	2
10	75,000	8
11	7,400	1

^aA simulated NMR dataset derived from the X-ray structure was used to constrain the analysis. The 26-residue peptide was divided into four-residue fragments with a two-residue overlap; backbone and side chain torsions were searched in 10 and 30 increments, respectively.



A summary of the number of conformations and families produced in this analysis is shown in Table 2. For several of the fragments, 75,000 or more conformations were found. These correspond to regions of the peptide having long side chains (for example Arg), which are often disordered in solution and as a result do not exhibit NOE information that would constrain the fragment search. In these cases, we set

an upper limit on the number of conformations and use a 'scramble' option in the creation of the trigonometric tables used during execution of the search. This randomizes the conformations that are evaluated and enhances sampling for regions of the molecule that are not well defined by the distance restraints. After intersection of the families shown in Table 2, four candidate structures were produced having a RMS distance versus the X-ray structure of 1.6–1.9 Å. Typically, a significant part of this deviation is innate to the geometries of the models employed. When a peptide is manually constructed from the amino acids model by setting the torsion angles to those observed in the X-ray structure, an RMS distance of approximately 1.0 Å is observed. A superimposition of the melittin X-ray structure and the closest Macrosearch structure (RMS distance = 1.693) is shown in Figure 8. The entire calculation took 1.5 h on a DEC Alpha 3000/300.

Macrosearch has been applied to several real NMR datasets, including emerimicin IV (Ac-Phe-MeA-MeA-MeA-Val-Gly-Leu-MeA-MeA-Hyp-Gln-EtA-Hyp-MeA-Phol; 47 rotatable bonds, about 200 NOE-based distance constraints, 15 $^3J_{\text{HH}}$ coupling constants, and nine hydrogen bonds)⁴¹ and a cyclic somatostatin analog {cyclo[Ala⁶-Tyr⁷-D-Trp⁸-Lys⁹-Val¹⁰-Phe¹¹-(CN₄)-]; 22 rotatable bonds, 27 distance restraints, five $J_{\text{NH-}\alpha\text{H}}$, and six $J_{\alpha\beta}$ }⁴².

Conclusions

Improvements in the speed and accuracy of systematic search have made it possible for us to address problems that ten years ago would have been intractable, or would have required an amount of time sufficient to compromise the utility of the results. Systematic conformational search as practiced now bears little resemblance to the integer, fixed grid sampling associated with its name. Our search protocols typically involve floating-point angle increments, which are unique to each torsion of a molecule, and we treat the grid as mutable and dynamic. Conformational searches are more accurate than at any point in the past, both because searches can be run with small grid sizes and because the reduced run time means numerous analyses can be done using different sets of adjustable parameters.

ACKNOWLEDGEMENTS

The authors acknowledge support from the National Institutes of Health (GM24483, Garland Marshall, P.I.) which has made the development of our systematic search software possible.

REFERENCES

- 1 Fesik, S.W. (1993) *J. Biomol. NMR* 3, 261–269
- 2 Greer, J. *et al.* (1994) *J. Med. Chem.* 37, 1035–1054
- 3 Bevan, P., Ryder, H. and Shaw, I. (1995) *Trends Biotechnol.* 13, 115–121
- 4 Kubinyi, H. (1995) *Pharmazie* 50, 647–662
- 5 Leach, A.R. (1991) in *Reviews in Computational Chemistry* (Vol. 2) (Lipkowitz, K.B. and Boyd, D.B., eds), pp. 1–55, VCH
- 6 Van Gunsteren, W.F. and Berendsen, H.J.C. (1990) *Angew. Chem., Int. Ed. Engl.* 29, 992–1023
- 7 Allen, M.P. and Tildesley, D.J. (1989) *Computer Simulation of Liquids*, Oxford Science Publications
- 8 Blaney, J.M. and Dixon, J.S. (1994) in *Reviews in Computational Chemistry* (Vol. 5) (Lipkowitz, K.B. and Boyd, D.B., eds), pp. 299–335, VCH
- 9 Leach, A.R., Prout, K. and Dolata, D.P. (1990) *J. Comput. Chem.* 11, 680–693
- 10 Motoc, I. *et al.* (1986) *Quant. Struct.-Act. Relatsh.* 5, 99–105
- 11 Moulton, J. and James, M.N.G. (1986) *Protein Struct. Funct. Genet.* 1, 146–163
- 12 Bruccoleri, R.E. and Karplus, M. (1987) *Biopolymers* 26, 137–168
- 13 Lipton, M. and Still, W.C. (1988) *J. Comput. Chem.* 9, 343–355
- 14 Iijima, H.I., Dunbar, J.B., Jr and Marshall, G.R. (1987) *Protein Struct. Funct. Genet.* 2, 330–339
- 15 Marshall, G.R. (1993) in *3D QSAR in Drug Design: Theory, Methods and Applications* (Kubinyi, H., ed.), pp. 80–116, ESCOM
- 16 Beusen, D.D. *et al.* *J. Mol. Struct.* (in press)
- 17 Dammkoehler, R.A. *et al.* (1989) *J. Comput.-Aided Mol. Design* 3, 3–21
- 18 Dammkoehler, R.A. *et al.* (1996) *J. Comput.-Aided Mol. Design* 9, 491–499
- 19 Marshall, G.R. *et al.* (1979) in *Computer-Assisted Drug Design* (Vol. 112) (Olson, E.C. and Christoffersen, R.E., eds), pp. 205–226, American Chemical Society
- 20 Mayer, D. *et al.* (1987) *J. Comput.-Aided Mol. Design* 1, 3–16
- 21 Waller, C.L. *et al.* *J. Comput.-Aided Mol. Design* (in press)
- 22 Regoli, D., Boudon, A. and Fauchere, J.L. (1994) *Pharmacol. Rev.* 46, 551–599
- 23 Lowe, J.A., III *et al.* (1992) *J. Med. Chem.* 35, 2591–2600
- 24 Desai, M.C. *et al.* (1992) *J. Med. Chem.* 35, 4911–4913
- 25 Lewis, R.T. *et al.* (1995) *J. Med. Chem.* 38, 923–933
- 26 Garret, C. *et al.* (1991) *Proc. Natl. Acad. Sci. U. S. A.* 88, 10208–10212
- 27 Cascieri, M.A. *et al.* (1994) *J. Biol. Chem.* 269, 6587–6591
- 28 Desai, M.C., Vincent, L.A. and Rizzi, J.P. (1994) *J. Med. Chem.* 37, 4263–4266
- 29 Cascieri, M.A. *et al.* (1995) *Mol. Pharmacol.* 47, 660–665
- 30 Howard, H.R., Shenk, K.D. and Coffman, K.C. (1995) *Bioorg. Med. Chem. Lett.* 5, 111–114
- 31 Kataoka, T. *et al.* (1992) *Biopolymers* 32, 1519–1533
- 32 Peishoff, C.E., Dixon, J.S. and Kopple, K.D. (1990) *Biopolymers* 30, 45–56
- 33 Saunders, M. *et al.* (1990) *J. Am. Chem. Soc.* 112, 1419–1427
- 34 Saunders, M. and Jimenez-Vazquez, H.A. (1993) *J. Comput. Chem.* 14, 330–348
- 35 Bohm, H.-J. *et al.* (1990) *J. Comput. Chem.* 11, 1021–1028
- 36 Peishoff, C.E. and Dixon, J.S. (1992) *J. Comput. Chem.* 13, 565–569
- 37 Cambridge Structural Database System 3, Cambridge Crystallographic Data Centre, 12 Union Road, Cambridge, UK CB2 1EZ
- 38 Guntert, P. *et al.* (1989) *J. Am. Chem. Soc.* 111, 3997–4004
- 39 Nilges, M., Clore, G.M. and Gronenborn, A.M. (1990) *Biopolymers* 29, 813–822
- 40 Terwilliger, T.C. and Eisenberg, D. (1982) *J. Biol. Chem.* 257, 6010–6015
- 41 Beusen, D.D. *et al.* (1992) in *Peptides 1992 (22nd European Peptide Symposium)* (Schneider, C.H. and Eberle, A.N., eds), pp. 79–80, ESCOM
- 42 Beusen, D.D. *et al.* (1995) *Biopolymers* 36, 181–200